Radiology Research and Practice

Oral and Maxillofacial Imaging for the Diagnosis of Systemic Diseases in Dentistry

Lead Guest Editor: Mahin Bakhshi
Guest Editors: Maryam Tofangchiha, Sedigheh Bakhtiari, and Filiz Namdar Pekiner

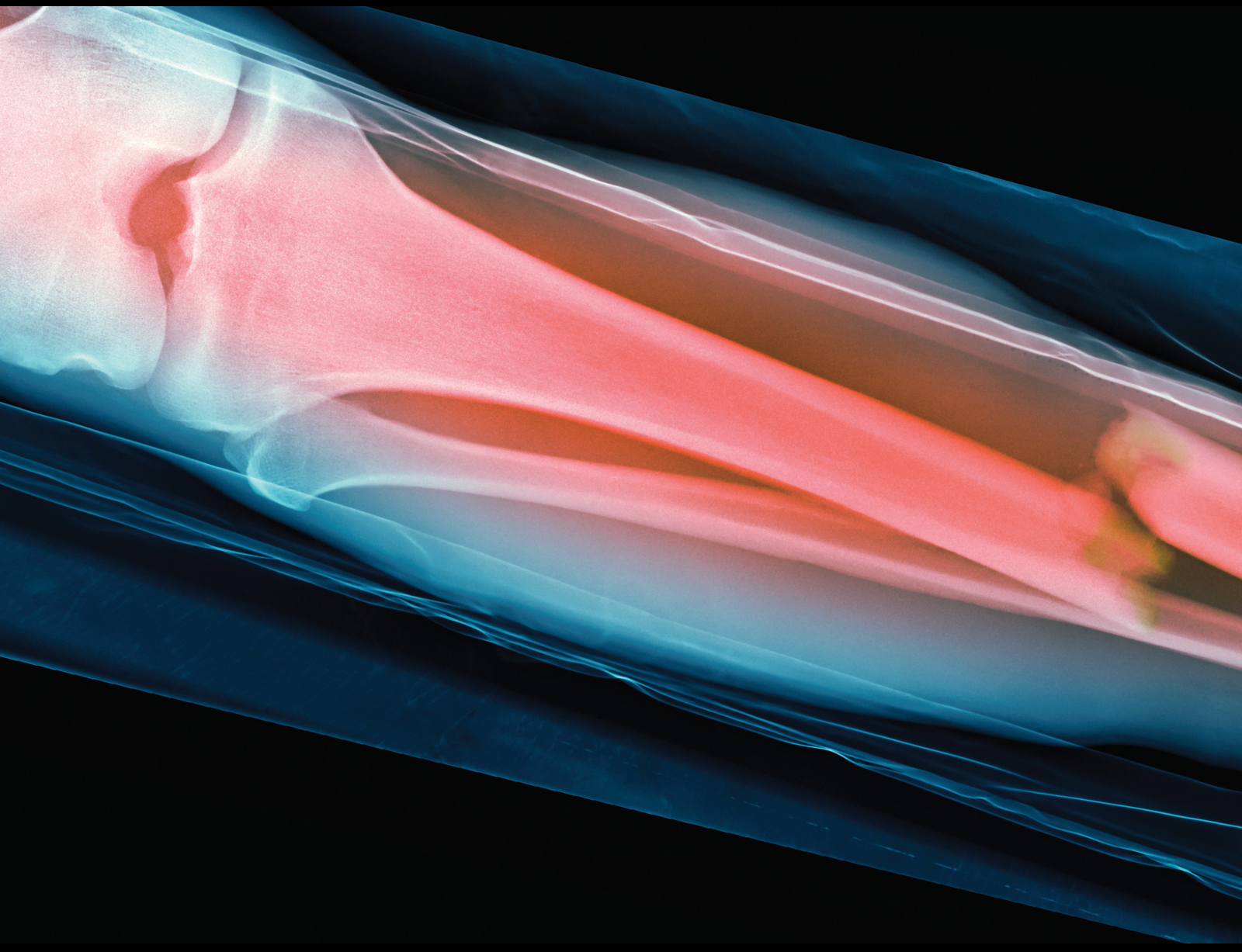

Oral and Maxillofacial Imaging for the Diagnosis of Systemic Diseases in Dentistry

Radiology Research and Practice

Oral and Maxillofacial Imaging for the Diagnosis of Systemic Diseases in Dentistry

Lead Guest Editor: Mahin Bakhshi
Guest Editors: Maryam Tofangchiha, Sedigheh Bakhtiari, and Filiz Namdar Pekiner

Academic Editors

Contents

Hindawi
Radiology Research and Practice
Volume 2022, Article ID 1614838, 10 pages
https://doi.org/10.1155/2022/1614838

Review Article

Oral Cancer Screening by Artificial Intelligence-Oriented Interpretation of Optical Coherence Tomography Images

Kousar Ramezani and Maryam Tofangchiha

Department of Oral and Maxillofacial Radiology, Dental Caries Prevention Research Center, Qazvin University of Medical Sciences, Qazvin, Iran

Correspondence should be addressed to Maryam Tofangchiha; mt_tofangchiha@yahoo.com

Received 26 November 2021; Revised 23 March 2022; Accepted 11 April 2022; Published 23 April 2022

Academic Editor: André Luiz Ferreira Costa

Early diagnosis of oral cancer is critical to improve the survival rate of patients. The current strategies for screening of patients for oral premalignant and malignant lesions unfortunately miss a significant number of involved patients. Optical coherence tomography (OCT) is an optical imaging modality that has been widely investigated in the field of oncology for identification of cancerous entities. Since the interpretation of OCT images requires professional training and OCT images contain information that cannot be inferred visually, artificial intelligence (AI) with trained algorithms has the ability to quantify visually undetectable variations, thus overcoming the barriers that have postponed the involvement of OCT in the process of screening of oral neoplastic lesions. This literature review aimed to highlight the features of precancerous and cancerous oral lesions on OCT images and specify how AI can assist in screening and diagnosis of such pathologies.

1. Introduction

Medical imaging is an inseparable part of medical diagnosis and plays a pivotal role in cancer screening and follow-up of treatments. In the specific field of oncology, imaging provides valuable anatomical and functional information that can preciously improve the results of screening, diagnosis, treatment, and follow-up [1]. Computed tomography (CT), magnetic resonance imaging (MRI), ultrasonography, positron emission tomography, single photon emission CT, and other modalities are utilized to detect tumoral changes. However, none of these modalities can address all aspects of a cancer diagnosis. CT, MRI, and ultrasonography provide structural information about the tumors, such as their location and extension; meanwhile positron emission tomography and single photon emission CT reveal functional and molecular information [2]. Besides, there are still demands to improve spatial and contrast resolutions of these modalities to provide more accurate information [1, 3].

Early diagnosis of tumoral changes not only ensures appropriate timing for surgical intervention and subsequent treatment and increases the survival rate but also decreases postsurgical morbidity, especially in invasive and malignant tumors, because less tissues are involved. Definite cancer diagnosis relies on histopathological assessment that requires tissue preparation and is time-consuming. Moreover, in large tumors, several samples from different sites need to be excised. Besides, in the process of surgical removal of a tumor, surgeons need to examine the excised margins several times to ensure leaving clear and tumor-free margins. In such cases, immediate and precise histopathological examination may not be practically possible [4]. Artificial intelligence (AI) could be important as an auxiliary diagnostic tool due to the fact that intraoperative frozen sections are not ideal outcome predictors in certain locations [5]. Therefore, the use of computer science may be of assistance to noninvasively improve the accuracy of diagnosis.

Approximately 300,000 new cases of oral cancer are diagnosed annually worldwide which are responsible for over 145,000 deaths per year. Oral cancer ranks the sixth most common cancer worldwide, with an increasing incidence rate but constant survival rate during the past decades

because of delayed detection and reliance on traditional screening methods. The importance of early detection of oral cancer is further understood when comparing the 5-year survival rate of 80–90% in case of early diagnosis and treatment with 30% rate in cases diagnosed in advanced stages [6, 7]. Oral leukoplakia, erythroleukoplakia, and verrucous hyperplasia are precancerous lesions with the potential to transform into squamous cell carcinoma (SCC) [8]. SCC accounts for 90% of all oral malignancies [9]. Biopsy is the gold standard for oral cancer diagnosis; however, it is painful, and, in case of extensive or multiple lesions, site and size selection for surgical removal of biopsy sample is critical and sometimes confusing [10]. Moreover, the prepared histological specimen may not reflect the identity of the whole lesion due to lesion heterogeneity. Adjunctive methods to aid the clinicians in selecting the best site for biopsy decrease false-negative results [11].

Optical coherence tomography (OCT) is a noninvasive real-time imaging modality that delivers three-dimensional (3D) high-resolution microscale images (axial and lateral resolutions of 13–17 μm and 17–22 μm, respectively). An 8 μm axial resolution and a 2 μm axial and lateral resolution are reported as state of the art. OCT is fast, repeatable, and well tolerated by patients [12–14]. It has several potential applications in oncology. Real-time nondestructive high-resolution radiation-free OCT images make it an ideal modality for screening of neoplastic tissue changes. Moreover, it can aid in targeted biopsy, intraoperative surgical margin and lymph node histopathological assessments, and postoperative evaluation of treatment response, resulting in more successful tumor resection and improved survival rate [4]. Evidence shows that OCT images reveal helpful information for detection of early-stage oral cancer [15].

AI is affecting most aspects of human life; image-based medical diagnosis is not an exception. Screening of oral lesions relies on subjective interpretation of clinical features, which considerably varies in accuracy, sensitivity, and specificity as reported in the literature. Dentists are at the frontline of encountering cancerous lesions and have variable levels of diagnostic accuracy in detection of different lesions. Delayed referral to a specialist is a major cause of poor outcome of management of oral premalignant lesions [16–19]. AI enables easy access to specialized diagnosis specially in patients who cannot be referred to more equipped medical centers because of residing in remote localities or due to high transportation costs. Free software utilization can improve the accuracy of surgical treatment planning for oral cancer as well [20]. The recent COVID-19 pandemic proved the importance of technologies that eliminate the necessity of physical presence to receive services [21, 22]. The screening process for oral lesions currently lacks an accurate, nonsurgical, and reproducible imaging approach. Unfamiliar images for dental clinicians and a software environment that is difficult to interact for the operators are the main barriers against the widespread use of OCT for detection of oral lesions, despite its unique characteristics and high diagnostic value [16].

This literature review aims to summarize the features of oral precancerous and cancerous lesions on OCT images for medical and dental practitioners who are involved in diagnosis and treatment of these lesions and highlight how AI can improve the screening and diagnosis of such lesions.

2. Methods

A comprehensive search was conducted in PubMed for articles published in English up to August 28, 2021, using this query: (((optical coherence tomography) OR (OCT)) AND ((oral cancer*))) AND ((artificial intelligence) OR (machine learning) OR (deep learning) OR (convolutional neural network)). The inclusion criteria included studies that investigated oral precancerous or cancerous lesions on OCT images by any AI algorithm. Relevant articles were initially included based on their title and abstract and subsequently by their full text. The reference lists of relevant articles were also explored to find possibly missed articles.

2.1. OCT

2.1.1. Mechanism of Action. OCT uses a partially coherent near-infrared light beam of variable wavelength to image partially transparent tissues. The infrared wavelength (780–1550 nm) is a spectrum of light with deepest penetration into biological tissues (biological window) [23]. The beam reflected from the tissue layers produces an electric signal which can be detected afterwards. The term "tomography" implies the provided sections of the imaged object [24].

OCT consists of a broadband light source, an imaging system, a transducer, a data processor, and a computer to control the entire scanning process and image visualization [24]. The imaging principle of OCT is similar to that of ultrasonography. They both measure the backscattered beam emitted to the tissues, but, due to the differences in the wavelength and speed of light and acoustic waves, the penetration depth and the resolution they present are different. The mechanism of receiving the backscattered beam is fundamentally different as well [24]. The velocity of light is much higher than that of ultrasound waves; thus, measurement of time delay is impractical. Therefore, OCT utilizes an interferometer to calculate the pathway difference of light [25, 26]. The emitted beam is divided into the reference beam and sample beam which colligate again after reflection from the reference mirror and tissues, respectively. A photodetector or spectrometer records the interferences and digitizes them to be depicted graphically on a computer [27, 28]. The optical interfaces backscatter the emitted light with a time delay that is retrieved by Fourier transformation and used to calculate the distance between the optical reflections of tissue layers through interferometry resulting in A-scan sections. B-scan or longitudinal images employ a series of A-scans along a line on the x-axis and z-axis to create 2D views. C-scans or enface images are also 2D views obtained from the x-axis and y-axis. Volumetric data are reconstructed by 2D scanning of the layers [28–30].

The optical characteristics of a sample dictate the optical path and penetration depth of OCT beam, and OCT images reflect the coefficient of transmission information of a

sample [31]. The penetration depth declines as the density of the material increases [32]. Translucency of the medium determines the penetration depth as well [2, 19]. The axial resolution is defined by the wavelength and bandwidth of the light source [33].

OCT devices can be time-domain or frequency-domain devices based on their reference arm optics. The frequency-domain devices are of two types as well, spectral OCT and swept source OCT, based on the receiving compartments and output properties. The swept source OCT uses ultrahigh speed (kilohertz wavelength, center wavelength 1300 nm) laser beam which enhances the sensitivity of the system, penetration depth, resolution of the system, and scanning rate (1 second or less imaging speed), resulting in a shorter acquisition time [31, 34–37]. In the swept source OCT, the axial and transverse resolutions are determined by linewidth of the laser beam and focus spot size, respectively [23].

OCT can accompany probes and catheters to image internal organs and structures [4]. It should be noticed that mechanical compression of OCT probe on the soft tissue alters the optical properties of the tissue layers, increases the contrast between the layers, and decreases the thickness of the layers [38].

Although OCT is fundamentally a label-free modality, different contrast agents are studied to target specific cells or tissues including magnetic nanoparticles, gold nanoparticles, and encapsulating protein-shell microspheres [39–44]. Vessels could be detected on OCT images based on signal changes of light without additional contrast agents or dyes [45]. A study conducted to image the sublingual microcirculation found OCT to be suitable for this purpose [46]. A significant correlation has also been reported between histological slides and OCT images [10].

2.1.2. Dental Applications. OCT has proven its novel capabilities in some fields of medicine such as ophthalmology and cardiology; however, it has not been widely used in dentistry. OCT has been employed as a valuable tool for assessment of the anterior part of the visual pathway, optic nerve characterization, and visualization of cellular layers of macula [47]. Functional blood vessels of the eyes can be three-dimensionally reconstructed by OCT angiography based on its ability to detect moving red blood cells, which induce variations in the OCT signal [48]. OCT has been widely studied for detection of skin cancers and cutaneous inflammatory diseases based on its ability in imaging of skin tissue layers and substructures [49–51]. The hard and soft tissues of the maxillofacial region need a wide range of OCT rays. The scattering properties of wavelengths below 1000 nm match the dimensions of tissue particles, resulting in more efficient imaging. The tissues with higher water content dissipate the energy of the beam more; consequently, hard and soft tissues require adjusted wavelengths to obtain the best images [52]. Nontransparent tissues limit the penetration of OCT beam because of absorption and scattering effects [4]. OCT has higher penetration depth in comparison with the majority of optical imaging modalities [53–55].

Different sites of the oral cavity and hard-to-reach areas require customized applicable probes. For some pathological lesions, greater depth and a larger field of view may be required for a more comprehensive assessment of the tissues [56, 57].

The first designed OCT device for dental applications was hoped to be used for imaging of gingival margins, periodontal attachments, and pockets [58]. OCT has been used for evaluation of caries, propagation of demineralization or remineralization process, cracks, wear, erosion, deformations, age-related changes, restoration defects, root canal system, detection of pulp horns and isthmuses, sealing efficacy of cements, and evaluation of penetration depth of different materials into the tooth structure [59–65]. A unique superiority of OCT over the conventional X-ray examination for caries detection is visualization of incipient caries that could not be detected radiographically without radiation exposure. Radiography cannot distinguish active caries from arrested caries [24, 66]. Moreover, enamel and dentin could be easily differentiated on OCT images due to their different optical properties [12]. OCT shows promising results in pediatric dentistry for incipient caries detection due to its real-time and noninvasive nature [67]. In maxillofacial surgery, OCT can be used for soft tissue assessment and differentiation of normal tissue from dysplastic and malignant changes. Some studies used OCT to evaluate the periodontal tissues, peri-implant tissues, radiation-induced oral mucositis, and bullous lesions [68–72].

2.1.3. Oncological Applications. OCT does not have a large field of view or high penetration depth, but its micro-resolution and high soft tissue contrast due to differences in scattering properties make it an ideal nonsurgical modality to spatially differentiate cell layers and tissues. It has been widely used in oncological studies in vivo and in vitro [4, 73–75]. Visualization of microanatomy is not the only domain that OCT can shine in; it has been used to assess several cellular dynamics and cell processes that occur in premalignant and malignant tissues [76, 77]. Several OCT devices and probes have been commercialized for oncological applications [4].

Three-dimensional cell colonies are developed to aid in investigation of tumorigenesis mechanism and drug response with no need for animal models. OCT can monitor such samples periodically and repeatedly. It has been demonstrated that OCT has the ability to detect dead cells based on their scattering properties [78]. OCT is a good modality to monitor neoplastic changes in cellular scale and treatment response in 3D culture studies [76].

2.1.4. Cancer Indicators. Measurement of epithelial thickness on OCT images is valid, reliable, and practicable. The normal epithelial thickness is 75–550 μm in different sites and can be imaged by OCT with 2–3 mm penetration depth and 10–12 μm resolution [38, 79, 80]. The oral mucosa on OCT images is described as a hyporeflective epithelium underlined by the basement membrane and a hyperreflective lamina propria beneath them, containing blood vessels and

minor salivary glands [10]. The normal oral epithelium has a homogenous distribution of cells that are uniform in size and nucleus/plasma ratio, while this arrangement is impaired by cancer clusters and nests with variable cell sizes and nucleus/plasma ratio in cancerous epithelium [8].

Neoplastic changes are characterized by cells that are abnormal in shape and size and have enlarged nuclei. Such changes at the cellular and subcellular levels change the optical scattering properties of OCT, which enhances their detection. Some important histological indicators of malignancy in the epithelial tissue include expanded dysplastic cells, irregular epithelial stratification accompanied by broadened rete pegs, basal hyperplasia, and elongated papilla core [10, 81]. Dysplastic cells in the epithelium produce a dispersed speckle pattern on OCT B-scans [33]. Speckle formation is inevitable on OCT images because of the heterogeneous nature of the biological tissues which interferes with the optical beam in various levels [82].

Researchers have tried to find some indicators to differentiate intact, premalignant, and neoplastic tissues in epithelial mucosa, subepithelial tissue, and basement membrane of oral mucosa on OCT images. Thickening of basement membrane is a sign of tumor invasion and can be considered as an indicator of malignant changes. In a previous study, the mean epithelial layer thickness was the highest in microinvasive carcinoma, followed by carcinoma in situ, dysplasia, and benign lesions [83]. Another study confirmed increased thickness of epithelial layer after dysplastic changes, albeit the boundary between the epithelium and lamina propria, unlike SCC, could be delineated [84]. Tsai et al. considered epithelial thickness, the standard deviation of A-mode scan intensity profile, and the exponential decay constant of spatial-frequency spectrum of the A-mode scan profile as indicators to distinguish benign and malignant oral lesions [8, 84, 85]. They found that, in abnormal oral mucosal lesions, the standard deviation increased, the decay constant of the spatial-frequency spectrum decreased, and the epithelium thickness increased [8]. Neoangiogenesis, surface integrity, surface profile (even or uneven), epithelial homogeneity, loss of stratification in squamous epithelium, and tissue vascularization are other indicators as well [10, 86]. Neoplastic transformation can cause stromal changes, alter collagen and other extracellular components, or induce fibroblast proliferation [87, 88].

A clear boundary between the epithelium and lamina propria could not be identified on B-mode scans of cancerous lesions [8]. The epithelial thickness and basement membrane integrity are valid indicators to differentiate normal and dysplastic tissues, as well as invasive carcinoma [89]. The epithelial thickness increases prior to disappearance of lamina propria due to invasion of cancer cells [8].

The epithelial and subepithelial changes following dysplastic transformation result in stronger light scattering and fluctuation of spatial distribution. The mean intensity of spatial reflection is greater in dysplastic oral epithelium in comparison with normal tissue. Moreover, collagen deposition in lamina propria results in a reduction in SD level [85].

There is a distinctive contrast in signal intensity between the epithelium and lamina propria (bright epithelium and brighter lamina propria) in oral premalignant tissues; subsequently, this boundary can be precisely identified [85]. Lee et al. [85] used computer analysis to automatically differentiate normal and precancerous oral mucosa. They successfully plotted the boundary between the epithelium and lamina propria, measured the epithelial thickness, and estimated the range of dysplastic cell distribution.

2.1.5. AI. There are some drawbacks related to the oncological applications of OCT such as limited penetration depth, limited area and volume of scans, demand for higher resolution to visualize more cellular and subcellular details, too much noise, difficult image interpretation, and the training required for image interpretation [31]. Interpretation of OCT images is extremely operator-dependent, because there is no defined comprehensive and precise standard for interpretation of OCT images [30]. Interpretation of OCT images requires training and expertise, and since the configuration of OCT images is basically different from the conventional images, even medical imaging experts have difficulty in reading the OCT images. AI and machine learning algorithms can assist in interpretation of OCT images, providing fair and equal accessibility to an automated professional diagnosis with high accuracy [90]. Cutting-edge technologies introduced to the biomedical field might have too much presentable information and data, but as long as these datasets could not be precisely and efficiently translated to a clinical insight in a timely manner to affect the diagnosis and treatment outcome, they would be a waste of cost and time [91]. Deep learning algorithms and AI have not still found their appropriate clinical position despite their marvelous ability to increase the accuracy of interpretation and eliminate the efforts, cost, and time spent to train the operators [50].

Automatic processing of the features of OCT images not only saves the time of analyzing abundant volume of data but only will digitize the data that could not be interpreted subjectively [33]. Machine learning and deep learning are two subfields of AI. Machine learning algorithms need structured and labeled datasets; meanwhile deep learning algorithms generate their own subsets of data by identification of differences within layers of neural networks. Unlike the machine learning algorithms, deep learning algorithms require an abundant amount of data to build their network and perform their best [16]. Machine learning is fed by a large amount of ground truth manually labeled by the clinicians. Generation of expert-defined annotations is time-consuming and costly and is deteriorated by intergrader variability [92]. Deep learning has a multilayered convolutional neural network to learn and distinguish image features [93]. Deep learning enhances predictive accuracy by weight adjustment of data through a process called back-propagation [94]. It strengthens or weakens the weight of each synapse based on the input "answer" to reach the highest agreement. Deep learning diagnosis is built based on the multiblinded experts' decisions. If the introduced data to the algorithm are large enough, intergrader variability will not have a significant impact on evolution of training. A

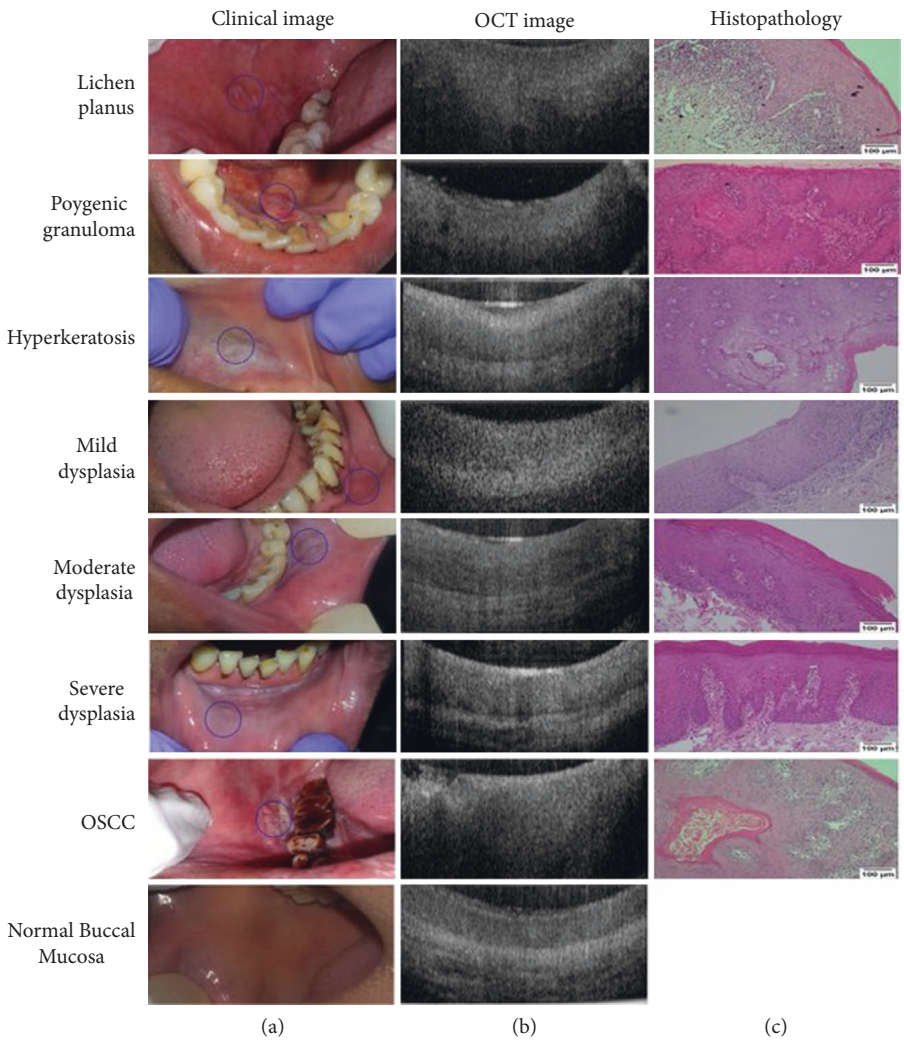

Figure 1: Clinical, OCT, and histological images. Clinical (a) and OCT (b) images were captured from all subjects, and biopsy samples were collected (wherever indicated) and assessed histopathologically (c). Histological images were taken at 100x resolution (scale bar = 100 μm) using Nikon DSFi2 and NIS elements D4 20.0. The nondysplastic lesions shown were histologically diagnosed with lichen planus, pyogenic granuloma, and hyperkeratosis. Normal buccal mucosa images were taken from a healthy volunteer without any habit history. Representative images of all dysplastic grades and a buccal oral squamous cell carcinoma (OSCC) are also depicted (image courtesy of https://bit.ly/316d1S1).

trained model might present unknown information, because it might recognize features that could not be detected by the operators [21, 95].

Artificial neural networks are machine learning algorithms made of associated working units known as neurons. The neurons are arranged in layers and acquire a value based on the activation frequency. When the neuron layers extend to more than 2–3 layers, it is known as deep learning artificial neural network. Deep learning convolution neural network is a model with multiple neural layers that administrate template-matching of input data with ground truth. Convolution neural network can be trained by continuous introduction of structured data and can upgrade its operation ability [96]. Convolutional neural networks are the most popular deep learning programs for analyzing visual figures [21]. Deeper number of convolutional layers and bridge connections between layers in deep learning algorithms bring about higher performance [82]. Even a minor sensitivity to variations in tissue characteristics might be sufficient for deep neural network architecture to diagnose alterations in the relevant image properties, a specialty that even an expert rater cannot reach visually [82]. Various neural network architectures are introduced for semantic segmentation process [97]. Manual image segmentation needs time and expertise and has variable reproducibility, and, in contrast to automated algorithms trained for this application, high-quality images are required [98].

Deep learning algorithms have shown promising results in ophthalmology such as macular edema detection, retinal thickness measurement, and retinal layer segmentation [95, 99–105]. They have been successfully used for compartmentalization of retinal layers with statistics comparable to the human grader [106]. Automated detection of basal cell carcinoma on OCT images has shown promising results with

excellent statistics of around 95% for accuracy, sensitivity, and specificity [90]. An automated segmentation algorithm can delineate the basement membrane and measure the epithelial thickness [107]. AI has been used to extract pathological features of CT, MRI, and endoscopy images [108–110]. Hwang et al. [21] designated a workflow for involvement of AI in the processing of OCT images for macula edema screening. Their workflow framework can be generalized to oral lesion screening on OCT images.

A marvelous preponderance of image translation by AI is that AI can quantify variations which could not be even detected by inspection. Specific characteristics of the tissue texture could not be quantified by the naked eye. Moreover, AI is able to integrate multiple data variables including imaging, geographical, clinical, pathological, and electronic health data as well as risk factors, resulting in a more comprehensive and analytical diagnosis [16].

Appending a diagnostic algorithm to the OCT system eliminates the operator training considerations as well as inter- and intraoperator diagnostic errors and nullifies subjectivity in interpretation of images. It can speed up the analysis of large amounts of datasets as well.

There are few studies that utilized computational algorithms for normal or cancerous tissue characterization [8, 85]. Lee et al. [85] used standard deviation of the intensity of OCT images to identify normal and dysplastic oral mucosa. Pande et al. [33] described algorithms to characterize morphological features on OCT B-scans of hamster cheek pouch. They evaluated aberration of layered structure of the epithelium and epithelial thickness, which are indicators of malignant transformation. Their algorithm showed 78.5%, 76.6%, and 87.8% sensitivity for diagnosis of benign, precancerous, and cancerous lesions, respectively, and 87.6%, 86.2%, and 94.3% specificity for the aforementioned lesions, respectively. These results were strongly suggestive of automated oral cancer detection on OCT images. James et al. [111] implemented artificial neural networks and a support vector machine model to annotate image features of OCT images obtained from the normal oral mucosa and benign and malignant lesions (Figure 1).

The statistics demonstrated that OCT-based diagnosis of malignant and dysplastic oral lesions integrated with AI had comparable results (93–96% sensitivity and 74–49% specificity) to the biopsy. Heidari et al. [112] deployed a convolution neural network to discriminate normal and abnormal head and neck mucosa on 3D OCT images. They reported 100%, 70%, and 82% sensitivity, specificity, and accuracy, respectively, for identification of cancer-positive images.

A cloud-based platform has been launched for remote machine learning of OCT image analysis that could be employed for analysis of tumor images. Open access to this platform will nourish the algorithms with more diverse data, leading to enhanced performance [106].

2.2. Limitations. High cost and limited availability limit the extensive application of OCT in the clinical setting, leading to less available necessary data to enrich and enhance AI algorithms. Affordable OCT devices not only provide accessibility to this modality but also would supply the image analysis algorithms with more datasets. Since the diagnosis of oral cancer and precancerous lesions, interpretation of OCT images, and development of AI algorithms for automated OCT image interpretation require profound expertise, qualified teams with experts from all related fields are required to collaborate interactively to achieve the desirable results. These requirements decrease the pace of employing AI algorithms in oral cancer screening and diagnosis by OCT images. Further studies are required to analyze and improve the efficiency and accuracy of AI algorithms for detection of cancerous changes before we could use such automated interpretation systems in the clinical setting.

3. Conclusion

AI algorithms have rendered hopeful outcomes in interpretation of OCT images of oral mucosa and discrimination of normal oral epithelium from precancerous and cancerous lesions. Progressive evolution of AI algorithms for interpretation of OCT images (which requires continuous data feed as ground information) paves the way towards automated oral cancer screening by OCT, even though it might be a long road to bring the integration of OCT and AI into the clinical setting. In addition to the need for further studies to provide OCT imaging data for AI algorithms, the existing challenges such as standardization of labeling, validation of automated interpretations, and development of infrastructures for application of AI in oral cancer screening and diagnosis must be addressed to enable the application of AI in OCT for the aforementioned purposes and enhance early detection of oral mucosal cancerous changes with no need for physical presence of experts.

Data Availability

This review article is supported by the data of previously reported in the studies and data sets which were cited.

Conflicts of Interest

The authors declare that they have no conflicts of interest.

References

[1] J. Czernin, M. Allen-Auerbach, and H. R. Schelbert, "Improvements in cancer staging with PET/CT: literature-based evidence as of September 2006," *Journal of Nuclear Medicine: Official Publication, Society of Nuclear Medicine*, vol. 48, no. 1, pp. 78S–88S, 2007.

[2] T. Derlin, V. Grünwald, J. Steinbach, H.-J. Wester, and T. L. Ross, "Molecular imaging in oncology using positron emission tomography," *Deutsches Ärzteblatt International*, vol. 115, no. 11, pp. 175–181, 2018.

[3] J. V. Frangioni, "New technologies for human cancer imaging," *Journal of Clinical Oncology*, vol. 26, no. 24, pp. 4012–4021, 2008.

[4] J. Wang, Y. Xu, and S. A. Boppart, "Review of optical coherence tomography in oncology," *Journal of Biomedical Optics*, vol. 22, no. 12, pp. 1–23, 2017.

[5] A. E. Walts and A. M. Marchevsky, "Current evidence does not warrant frozen section evaluation for the presence of tumor spread through alveolar spaces," *Archives of Pathology and Laboratory Medicine*, vol. 142, no. 1, pp. 59–63, 2018.

[6] C. Rivera, "Essentials of oral cancer," *International Journal of Clinical and Experimental Pathology*, vol. 8, no. 9, pp. 11884–11894, 2015.

[7] J. Walther, Q. Li, M. Villiger et al., "Depth-resolved birefringence imaging of collagen fiber organization in the human oral mucosa in vivo," *Biomedical Optics Express*, vol. 10, no. 4, pp. 1942–1956, 2019.

[8] M. T. Tsai, H. C. Lee, C. K. Lee et al., "Effective indicators for diagnosis of oral cancer using optical coherence tomography," *Optics Express*, vol. 16, no. 20, pp. 15847–15862, 2008.

[9] P. H. Montero and S. G. Patel, "Cancer of the oral cavity," *Surgical Oncology Clinics of North America*, vol. 24, no. 3, pp. 491–508, 2015.

[10] M. Albrecht, C. Schnabel, J. Mueller, J. Golde, E. Koch, and J. Walther, "In vivo endoscopic optical coherence tomography of the healthy human oral mucosa: qualitative and quantitative image analysis," *Diagnostics*, vol. 10, no. 10, 2020.

[11] A. Wan and N. Savage, "Biopsy and diagnostic histopathology in dental practice in Brisbane: usage patterns and perceptions of usefulness," *Australian Dental Journal*, vol. 55, no. 2, pp. 162–169, 2010.

[12] S. Ali, S. B. S. Gilani, J. Shabbir, K. S. Almulhim, A. Bugshan, and I. Farooq, "Optical coherence tomography's current clinical medical and dental applications: a review," *F1000 Research*, vol. 10, p. 310, 2021.

[13] C. Canavesi and J. P. Rolland, "Ten years of gabor-domain optical coherence microscopy," *Applied Sciences*, vol. 9, no. 12, 2019.

[14] L. van Manen, J. Dijkstra, C. Boccara et al., "The clinical usefulness of optical coherence tomography during cancer interventions," *Journal of Cancer Research and Clinical Oncology*, vol. 144, no. 10, pp. 1967–1990, 2018.

[15] J. Espigares, A. Sadr, H. Hamba et al., "Assessment of natural enamel lesions with optical coherence tomography in comparison with microfocus x-ray computed tomography," *Journal of Medical Imaging*, vol. 2, no. 1, Article ID 014001, 2015.

[16] B. Ilhan, K. Lin, P. Guneri, and P. Wilder-Smith, "Improving oral cancer outcomes with imaging and artificial intelligence," *Journal of Dental Research*, vol. 99, no. 3, pp. 241–248, 2020.

[17] R. Mehrotra and D. K. Gupta, "Exciting new advances in oral cancer diagnosis: avenues to early detection," *Head and Neck Oncology*, vol. 3, no. 1, p. 33, 2011.

[18] J. B. Epstein, P. Güneri, H. Boyacioglu, and E. Abt, "The limitations of the clinical oral examination in detecting dysplastic oral lesions and oral squamous cell carcinoma," *Journal of the American Dental Association*, vol. 143, no. 12, pp. 1332–1342, 2012.

[19] C. Grafton-Clarke, K. W. Chen, and J. Wilcock, "Diagnosis and referral delays in primary care for oral squamous cell cancer: a systematic review," *British Journal of General Practice*, vol. 69, no. 679, pp. e112–e126, 2019.

[20] J. P. P. Gomes, A. L. F. Costa, C. T. Chone, A. M. D. A. M. Altemani, J. M. C. Altemani, and C. S. P. Lima, "Three-dimensional volumetric analysis of ghost cell odontogenic carcinoma using 3-D reconstruction software: a case report," *Oral Surgery, Oral Medicine, Oral Pathology and Oral Radiology*, vol. 123, no. 5, pp. e170–e175, 2017.

[21] D.-K. Hwang, Y.-B. Chou, T.-C. Lin et al., "Optical coherence tomography-based diabetic macula edema screening with artificial intelligence," *Journal of the Chinese Medical Association*, vol. 83, no. 11, pp. 1034–1038, 2020.

[22] E. M. Sánchez-Morla, J. L. Fuentes, J. M. Miguel-Jiménez et al., "Automatic diagnosis of bipolar disorder using optical coherence tomography data and artificial intelligence," *Journal of Personalized Medicine*, vol. 11, no. 8, 2021.

[23] Y. Shimada, M. Yoshiyama, J. Tagami, and Y. Sumi, "Evaluation of dental caries, tooth crack, and age-related changes in tooth structure using optical coherence tomography," *Japanese Dental Science Review*, vol. 56, no. 1, pp. 109–118, 2020.

[24] M. Machoy, J. Seeliger, L. Szyszka-Sommerfeld, R. Koprowski, T. Gedrange, and K. Woźniak, "The use of optical coherence tomography in dental diagnostics: a state-of-the-art review," *Journal of Healthcare Engineering*, vol. 2017, Article ID 7560645, 31 pages, 2017.

[25] D. Huang, E. A. Swanson, C. P. Lin et al., "Optical coherence tomography," *Science*, vol. 254, no. 5035, pp. 1178–1181, 1991.

[26] J. G. Fujimoto, "Optical coherence tomography for ultrahigh resolution in vivo imaging," *Nature Biotechnology*, vol. 21, no. 11, pp. 1361–1367, 2003.

[27] T. O. Steele and A. Meyers, "Early detection of premalignant lesions and oral cancer," *Otolaryngologic Clinics of North America*, vol. 44, no. 1, pp. 221–229, 2011.

[28] Y.-S. Hsieh, Y.-C. Ho, S.-Y. Lee et al., "Dental optical coherence tomography," *Sensors*, vol. 13, no. 7, pp. 8928–8949, 2013.

[29] M.-T. Tsai, Y.-L. Wang, T.-W. Yeh et al., "Early detection of enamel demineralization by optical coherence tomography," *Scientific Reports*, vol. 9, no. 1, Article ID 17154, 2019.

[30] E. Gentile, C. Maio, A. Romano, L. Laino, and A. Lucchese, "The potential role of in vivo optical coherence tomography for evaluating oral soft tissue: a systematic review," *Journal of Oral Pathology & Medicine: Official Publication of the International Association of Oral Pathologists and the American Academy of Oral Pathology*, vol. 46, no. 10, pp. 864–876, 2017.

[31] H. Watanabe, A. Kuribayashi, Y. Sumi, and T. Kurabayashi, "Resolution characteristics of optical coherence tomography for dental use," *Dentomaxillofacial Radiology*, vol. 46, no. 3, Article ID 20160358, 2017.

[32] E. Ralph-Alexandru, D. Virgil-Florin, D. George, B. Adrian, and P. Adrian, "A combination of imaging techniques for dental medicine: from x-rays radiography and 3D CBCT to OCT," in *Proceedings of the SPIE Photonics Europe*, Strasbourg, France, 2020.

[33] P. Pande, S. Shrestha, J. Park et al., "Automated classification of optical coherence tomography images for the diagnosis of oral malignancy in the hamster cheek pouch," *Journal of Biomedical Optics*, vol. 19, no. 8, Article ID 086022, 2014.

[34] B. Potsaid, B. Baumann, D. Huang et al., "Ultrahigh speed 1050 nm swept source/fourier domain OCT retinal and anterior segment imaging at 100,000 to 400,000 axial scans per second," *Optics Express*, vol. 18, no. 19, pp. 20029–20048, 2010.

[35] K. J. Mohler, W. Draxinger, T. Klein et al., "Combined 60° wide-field choroidal thickness maps and high-definition en face vasculature visualization using swept-source megahertz

OCT at 1050 nm," *Investigative Opthalmology and Visual Science*, vol. 56, no. 11, pp. 6284–6293, 2015.

[36] M. N. Luong, Y. Shimada, K. Araki, M. Yoshiyama, J. Tagami, and A. Sadr, "Diagnosis of occlusal caries with dynamic slicing of 3D optical coherence tomography images," *Sensors*, vol. 20, no. 6, 2020.

[37] F. C. M. Suassuna, A. M. A. Maia, D. P. Melo, A. C. D. Antonino, A. S. L. Gomes, and P. M. Bento, "Comparison of microtomography and optical coherence tomography on apical endodontic filling analysis," *Dentomaxillofacial Radiology*, vol. 47, no. 2, Article ID 20170174, 2018.

[38] D. Di Stasio, D. Lauritano, F. Loffredo et al., "Optical coherence tomography imaging of oral mucosa bullous diseases: a preliminary study," *Dentomaxillofacial Radiology*, vol. 49, no. 2, Article ID 20190071, 2020.

[39] R. John, F. T. Nguyen, K. J. Kolbeck et al., "Targeted multifunctional multimodal protein-shell microspheres as cancer imaging contrast agents," *Molecular Imaging and Biology*, vol. 14, no. 1, pp. 17–24, 2012.

[40] T. M. Lee, A. L. Oldenburg, S. Sitafalwalla et al., "Engineered microsphere contrast agents for optical coherence tomography," *Optics Letters*, vol. 28, no. 17, pp. 1546–1548, 2003.

[41] C. Xu, J. Ye, D. L. Marks, and S. A. Boppart, "Near-infrared dyes as contrast-enhancing agents for spectroscopic optical coherence tomography," *Optics Letters*, vol. 29, no. 14, pp. 1647–1649, 2004.

[42] H. Cang, T. Sun, Z.-Y. Li et al., "Gold nanocages as contrast agents for spectroscopic optical coherence tomography," *Optics Letters*, vol. 30, no. 22, pp. 3048–3050, 2005.

[43] A. L. Oldenburg, M. N. Hansen, T. S. Ralston, A. Wei, and S. A. Boppart, "Imaging gold nanorods in excised human breast carcinoma by spectroscopic optical coherence tomography," *Journal of Materials Chemistry*, vol. 19, no. 35, p. 6407, 2009.

[44] M. C. Skala, M. J. Crow, A. Wax, and J. A. Izatt, "Photothermal optical coherence tomography of epidermal growth factor receptor in live cells using immunotargeted gold nanospheres," *Nano Letters*, vol. 8, no. 10, pp. 3461–3467, 2008.

[45] M.-T. Tsai, Y. Chen, C.-Y. Lee et al., "Noninvasive structural and microvascular anatomy of oral mucosae using handheld optical coherence tomography," *Biomedical Optics Express*, vol. 8, no. 11, pp. 5001–5012, 2017.

[46] M. Hessler, P. Nelis, C. Ertmer et al., "Optical coherence tomography angiography as a novel approach to contactless evaluation of sublingual microcirculation: a proof of principle study," *Scientific Reports*, vol. 10, no. 1, p. 5408, 2020.

[47] N. Minakaran, E. R. de Carvalho, A. Petzold, and S. H. Wong, "Optical coherence tomography (OCT) in neuro-ophthalmology," *Eye*, vol. 35, no. 1, pp. 17–32, 2021.

[48] A. Koustenis Jr., A. Harris, J. Gross, I. Januleviciene, A. Shah, and B. Siesky, "Optical coherence tomography angiography: an overview of the technology and an assessment of applications for clinical research," *British Journal of Ophthalmology*, vol. 101, no. 1, pp. 16–20, 2017.

[49] S. Chen, F. Xie, T. Hao et al., "Evaluation of ultrahigh-resolution optical coherence tomography for basal cell carcinoma, seborrheic keratosis, and nevus," *Skin Research and Technology*, vol. 27, no. 4, pp. 479–485, 2021.

[50] B. Wan, C. Ganier, X. Du-Harpur et al., "Applications and future directions for optical coherence tomography in dermatology*," *British Journal of Dermatology*, vol. 184, no. 6, pp. 1014–1022, 2021.

[51] C. Ruini, S. Schuh, E. Sattler, and J. Welzel, "Line-field confocal optical coherence tomography-practical applications in dermatology and comparison with established imaging methods," *Skin Research and Technology*, vol. 27, no. 3, pp. 340–352, 2021.

[52] A. M. A. Maia, A. Z. de Freitas, D. L C. Sergio, A. S. L. Gomes, and L. Karlsson, "Evaluation of dental enamel caries assessment using quantitative light induced fluorescence and optical coherence tomography," *Journal of Biophotonics*, vol. 9, no. 6, pp. 596–602, 2016.

[53] H. Wang, U. Baran, and R. K. Wang, "In vivo blood flow imaging of inflammatory human skin induced by tape stripping using optical microangiography," *Journal of Biophotonics*, vol. 8, no. 3, pp. 265–272, 2015.

[54] O. C. Raffel, T. Akasaka, and I.-K. Jang, "Cardiac optical coherence tomography," *Heart*, vol. 94, no. 9, pp. 1200–1210, 2008.

[55] L. M. Sakata, J. Deleon-Ortega, V. Sakata, and C. A. Girkin, "Optical coherence tomography of the retina and optic nerve—a review," *Clinical and Experimental Ophthalmology*, vol. 37, no. 1, pp. 90–99, 2009.

[56] K. Kikuchi, N. Akiba, A. Sadr, Y. Sumi, J. Tagami, and S. Minakuchi, "Evaluation of the marginal fit at implant-abutment interface by optical coherence tomography," *Journal of Biomedical Optics*, vol. 19, no. 5, Article ID 055002, 2014.

[57] C. C. B. O. Mota, L. O. Fernandes, R. Cimões, and A. S. L. Gomes, "Non-invasive periodontal probing through fourier-domain optical coherence tomography," *Journal of Periodontology*, vol. 86, no. 9, pp. 1087–1094, 2015.

[58] L. L. Otis, M. J. Everett, U. S. Sathyam, and B. W. Colston Jr, "Optical coherence tomography: a new imaging technology for dentistry," *Journal of the American Dental Association*, vol. 131, no. 4, pp. 511–514, 2000.

[59] D. Fried, J. Xie, S. Shafi, J. D. B. Featherstone, T. M. Breunig, and C. Le, "Imaging caries lesions and lesion progression with polarization sensitive optical coherence tomography," *Journal of Biomedical Optics*, vol. 7, no. 4, pp. 618–627, 2002.

[60] R. S. Jones, C. L. Darling, J. D. B. Featherstone, and D. Fried, "Remineralization of in vitro dental caries assessed with polarization-sensitive optical coherence tomography," *Journal of Biomedical Optics*, vol. 11, no. 1, Article ID 014016, 2006.

[61] T. M. S. Arnaud, B. de Barros Neto, and F. B. Diniz, "Chitosan effect on dental enamel de-remineralization: an in vitro evaluation," *Journal of Dentistry*, vol. 38, no. 11, pp. 848–852, 2010.

[62] A. Turkistani, A. Sadr, Y. Shimada, T. Nikaido, Y. Sumi, and J. Tagami, "Sealing performance of resin cements before and after thermal cycling: evaluation by optical coherence tomography," *Dental Materials*, vol. 30, no. 9, pp. 993–1004, 2014.

[63] Y. Iino, A. Ebihara, T. Yoshioka et al., "Detection of a second mesiobuccal canal in maxillary molars by swept-source optical coherence tomography," *Journal of Endodontics*, vol. 40, no. 11, pp. 1865–1868, 2014.

[64] B. Rashed, Y. Iino, K. Komatsu et al., "Evaluation of root canal anatomy of maxillary premolars using swept-source optical coherence tomography in comparison with dental operating microscope and cone beam computed tomography," *Photomedicine and Laser Surgery*, vol. 36, no. 9, pp. 487–492, 2018.

[65] R. A. Erdelyi, V. F. Duma, C. Sinescu, G. M. Dobre, A. Bradu, and A. Podoleanu, "Dental diagnosis and treatment

assessments: between x-rays radiography and optical coherence tomography," *Materials*, vol. 13, no. 21, 2020.

[66] J. Gomez, "Detection and diagnosis of the early caries lesion," *BMC Oral Health*, vol. 15, no. 1, p. S3, 2015.

[67] A. M. A. Maia, D. D. D. Fonsêca, B. B. C. Kyotoku, and A. S. L. Gomes, "Characterization of enamel in primary teeth by optical coherence tomography for assessment of dental caries," *International Journal of Paediatric Dentistry*, vol. 20, no. 2, pp. 158–164, 2010.

[68] O. K. Adegun, P. H. Tomlins, E. Hagi-Pavli, D. L. Bader, and F. Fortune, "Quantitative optical coherence tomography of fluid-filled oral mucosal lesions," *Lasers in Medical Science*, vol. 28, no. 5, pp. 1249–1255, 2013.

[69] O. K. Adegun, P. H. Tomlins, E. Hagi-Pavli et al., "Quantitative analysis of optical coherence tomography and histopathology images of normal and dysplastic oral mucosal tissues," *Lasers in Medical Science*, vol. 27, no. 4, pp. 795–804, 2012.

[70] M. Sanda, M. Shiota, C. Imakita, A. Sakuyama, S. Kasugai, and Y. Sumi, "The effectiveness of optical coherence tomography for evaluating peri-implant tissue: a pilot study," *Imaging Science in Dentistry*, vol. 46, no. 3, pp. 173–178, 2016.

[71] T. M. Muanza, A. P. Cotrim, M. McAuliffe et al., "Evaluation of radiation-induced oral mucositis by optical coherence tomography," *Clinical Cancer Research*, vol. 11, no. 14, pp. 5121–5127, 2005.

[72] P. Wilder-Smith, M. J. Hammer-Wilson, J. Zhang et al., "In vivo imaging of oral mucositis in an animal model using optical coherence tomography and optical doppler tomography," *Clinical Cancer Research*, vol. 13, no. 8, pp. 2449–2454, 2007.

[73] C. Kut, K. L. Chaichana, J. Xi et al., "Detection of human brain cancer infiltration ex vivo and in vivo using quantitative optical coherence tomography," *Science Translational Medicine*, vol. 7, no. 292, Article ID 292ra100, 2015.

[74] S. J. Erickson-Bhatt, R. M. Nolan, N. D. Shemonski et al., "Real-time imaging of the resection bed using a handheld probe to reduce incidence of microscopic positive margins in cancer surgery," *Cancer Research*, vol. 75, no. 18, pp. 3706–3712, 2015.

[75] C. S. Kim, P. Wilder-Smith, Y.-C. Ahn, L.-H. L. Liaw, Z. Chen, and Y. J. Kwon, "Enhanced detection of early-stage oral cancer in vivo by optical coherence tomography using multimodal delivery of gold nanoparticles," *Journal of Biomedical Optics*, vol. 14, no. 3, Article ID 034008, 2009.

[76] Y.-Z. Liu, N. D. Shemonski, S. G. Adie et al., "Computed optical interferometric tomography for high-speed volumetric cellular imaging," *Biomedical Optics Express*, vol. 5, no. 9, pp. 2988–3000, 2014.

[77] R. K. Chhetri, Z. F. Phillips, M. A. Troester, and A. L. Oldenburg, "Longitudinal study of mammary epithelial and fibroblast co-cultures using optical coherence tomography reveals morphological hallmarks of pre-malignancy," *PLoS One*, vol. 7, no. 11, Article ID e49148, 2012.

[78] Y. Huang, S. Wang, Q. Guo et al., "Optical coherence tomography detects necrotic regions and volumetrically quantifies multicellular tumor spheroids," *Cancer Research*, vol. 77, no. 21, pp. 6011–6020, 2017.

[79] A. Mamalis, D. Ho, and J. Jagdeo, "Optical coherence tomography imaging of normal, chronologically aged, photoaged and photodamaged skin," *Dermatologic Surgery*, vol. 41, no. 9, pp. 993–1005, 2015.

[80] S. Prestin, S. I. Rothschild, C. S. Betz, and M. Kraft, "Measurement of epithelial thickness within the oral cavity using optical coherence tomography," *Head and Neck*, vol. 34, no. 12, pp. 1777–1781, 2012.

[81] P. H. Chen, H. Y. Lee, Y. F. Chen et al., "Detection of oral dysplastic and early cancerous lesions by polarization-sensitive optical coherence tomography," *Cancers*, vol. 12, no. 9, 2020.

[82] C. S. Lee, A. J. Tyring, Y. Wu et al., "Generating retinal flow maps from structural optical coherence tomography with artificial intelligence," *Scientific Reports*, vol. 9, no. 1, p. 5694, 2019.

[83] Z. Hamdoon, W. Jerjes, T. Upile, G. McKenzie, A. Jay, and C. Hopper, "Optical coherence tomography in the assessment of suspicious oral lesions: an immediate ex vivo study," *Photodiagnosis and Photodynamic Therapy*, vol. 10, no. 1, pp. 17–27, 2013.

[84] M.-T. Tsai, C.-K. Lee, H.-C. Lee et al., "Differentiating oral lesions in different carcinogenesis stages with optical coherence tomography," *Journal of Biomedical Optics*, vol. 14, no. 4, Article ID 044028, 2009.

[85] C.-K. Lee, T.-T. Chi, C.-T. Wu, M.-T. Tsai, C.-P. Chiang, and C.-C. Yang, "Diagnosis of oral precancer with optical coherence tomography," *Biomedical Optics Express*, vol. 3, no. 7, pp. 1632–1646, 2012.

[86] U. H. Ansari, E. Wong, M. Smith et al., "Validity of narrow band imaging in the detection of oral and oropharyngeal malignant lesions: a systematic review and meta-analysis," *Head and Neck*, vol. 41, no. 7, pp. 2430–2440, 2019.

[87] A. Devendra, K. C. Niranjan, A. Swetha, and H. Kaveri, "Histochemical analysis of collagen reorganization at the invasive front of oral squamous cell carcinoma tumors," *Journal of Investigative and Clinical Dentistry*, vol. 9, no. 1, 2018.

[88] G. W. Gynther, B. Rozell, and A. Heimdahl, "Direct oral microscopy and its value in diagnosing mucosal lesions," *Oral Surgery, Oral Medicine, Oral Pathology, Oral Radiology and Endodontics*, vol. 90, no. 2, pp. 164–170, 2000.

[89] D. D. Stasio, D. Lauritano, H. Iquebal, A. Romano, E. Gentile, and A. Lucchese, "Measurement of oral epithelial thickness by optical coherence tomography," *Diagnostics*, vol. 9, no. 3, 2019.

[90] T. Marvdashti, L. Duan, S. Z. Aasi, J. Y. Tang, and A. K. Ellerbee Bowden, "Classification of basal cell carcinoma in human skin using machine learning and quantitative features captured by polarization sensitive optical coherence tomography," *Biomedical Optics Express*, vol. 7, no. 9, pp. 3721–3735, 2016.

[91] G. Litscher, "Innovation in medicine," *Medicine*, vol. 1, no. 1, pp. 1-2, 2014.

[92] H. Valizadegan, Q. Nguyen, and M. Hauskrecht, "Learning classification models from multiple experts," *Journal of Biomedical Informatics*, vol. 46, no. 6, pp. 1125–1135, 2013.

[93] Y. LeCun, Y. Bengio, and G. Hinton, "Deep learning," *Nature*, vol. 521, no. 7553, pp. 436–444, 2015.

[94] V. Gulshan, L. Peng, M. Coram et al., "Development and validation of a deep learning algorithm for detection of diabetic retinopathy in retinal fundus photographs," *JAMA*, vol. 316, no. 22, pp. 2402–2410, 2016.

[95] S. Kuwayama, Y. Ayatsuka, D. Yanagisono et al., "Automated detection of macular diseases by optical coherence tomography and artificial intelligence machine learning of optical coherence tomography images," *Journal of Ophthalmology*, vol. 2019, Article ID 6319581, 2019.

[96] M. A. Mazurowski, M. Buda, A. Saha, and M. R. Bashir, "Deep learning in radiology: an overview of the concepts and

a survey of the state of the art with focus on MRI," *Journal of Magnetic Resonance Imaging*, vol. 49, no. 4, pp. 939–954, 2019.

[97] E. Shelhamer, J. Long, and T. Darrell, "Fully convolutional networks for semantic segmentation," *IEEE Transactions on Pattern Analysis and Machine Intelligence*, vol. 39, no. 4, pp. 640–651, 2017.

[98] J. Ho, M. Adhi, C. Baumal et al., "Agreement and reproducibility of retinal pigment epithelial detachment volumetric measurements through optical coherence tomography," *Retina*, vol. 35, no. 3, pp. 467–472, 2015.

[99] J. J. Titano, M. Badgeley, J. Schefflein et al., "Automated deep-neural-network surveillance of cranial images for acute neurologic events," *Nature Medicine*, vol. 24, no. 9, pp. 1337–1341, 2018.

[100] J. De Fauw, J. R. Ledsam, B. Romera-Paredes et al., "Clinically applicable deep learning for diagnosis and referral in retinal disease," *Nature Medicine*, vol. 24, no. 9, pp. 1342–1350, 2018.

[101] S. K. Devalla, K. S. Chin, J.-M. Mari et al., "A deep learning approach to digitally stain optical coherence tomography images of the optic nerve head," *Investigative Opthalmology and Visual Science*, vol. 59, no. 1, pp. 63–74, 2018.

[102] C. S. Lee, A. J. Tyring, N. P. Deruyter, Y. Wu, A. Rokem, and A. Y. Lee, "Deep-learning based, automated segmentation of macular edema in optical coherence tomography," *Biomedical Optics Express*, vol. 8, no. 7, pp. 3440–3448, 2017.

[103] T. Schlegl, S. M. Waldstein, H. Bogunovic et al., "Fully automated detection and quantification of macular fluid in OCT using deep learning," *Ophthalmology*, vol. 125, no. 4, pp. 549–558, 2018.

[104] L. Fang, D. Cunefare, C. Wang, R. H. Guymer, S. Li, and S. Farsiu, "Automatic segmentation of nine retinal layer boundaries in OCT images of non-exudative AMD patients using deep learning and graph search," *Biomedical Optics Express*, vol. 8, no. 5, pp. 2732–2744, 2017.

[105] F. G. Venhuizen, B. van Ginneken, B. Liefers et al., "Robust total retina thickness segmentation in optical coherence tomography images using convolutional neural networks," *Biomedical Optics Express*, vol. 8, no. 7, pp. 3292–3316, 2017.

[106] P. M. Maloca, A. Y. Lee, E. R. de Carvalho et al., "Validation of automated artificial intelligence segmentation of optical coherence tomography images," *PLoS One*, vol. 14, no. 8, Article ID e0220063, 2019.

[107] N. G. Ryan, M. D. L. Anthony, C. Lucas et al., "Automated segmentation of oral mucosa from wide-field OCT Images (Conference Presentation)," in *Proceedings of the Advanced Biomedical and Clinical Diagnostic and Surgical Guidance Systems*, San Francisco, CA, USA, 2016.

[108] D. Nie, X. Cao, Y. Gao, L. Wang, and D. Shen, "Estimating CT image from MRI data using 3D fully convolutional networks," *Deep Learning and Data Labeling for Medical Applications*, vol. 2016, pp. 170–178, 2016.

[109] M. van Stralen, Y. Zhou, P. Wozny, P. R. Seevinck, and M. Loog, "Contextual loss functions for optimization of convolutional neural networks generating pseudo CTs from MRI," *Medical Imaging 2018: Image Processing*, International Society for Optics and Photonics, Bellingham, WA, USA, 2018.

[110] A. P. Leynes, J. Yang, F. Wiesinger et al., "Direct pseudoCT generation for pelvis PET/MRI attenuation correction using deep convolutional neural networks with multi-parametric MRI: zero echo-time and Dixon deep pseudoCT (ZeDD-CT)," *Journal of Nuclear Medicine*, vol. 59, 2017.

[111] B. L. James, S. P. Sunny, A. E. Heidari et al., "Validation of a point-of-care optical coherence tomography device with machine learning algorithm for detection of oral potentially malignant and malignant lesions," *Cancers*, vol. 13, no. 14, 2021.

[112] A. E. Heidari, T. T. Pham, I. Ifegwu et al., "The use of optical coherence tomography and convolutional neural networks to distinguish normal and abnormal oral mucosa," *Journal of Biophotonics*, vol. 13, no. 3, Article ID e201900221, 2020.

Hindawi
Radiology Research and Practice
Volume 2021, Article ID 6097795, 5 pages
https://doi.org/10.1155/2021/6097795

Research Article

Occurrence of the Elongated Styloid Process on Digital Panoramic Radiographs in the Riyadh Population

Lingam Amara Swapna,[1] **Nada Tarek AlMegbil**,[1] **Alhanouf Othman Almutlaq**,[1] **and Pradeep Koppolu**[2]

[1]*Department of Surgical and Diagnostic Sciences, College of Dentistry, Dar Al Uloom University, Riyadh 13314, Saudi Arabia*
[2]*Department of Preventive Dental Sciences, College of Dentistry, Dar Al Uloom University, Riyadh 13314, Saudi Arabia*

Correspondence should be addressed to Lingam Amara Swapna; laswapna123@gmail.com

Received 24 August 2021; Revised 9 October 2021; Accepted 26 October 2021; Published 11 November 2021

Academic Editor: Maryam Tofangchiha

Background. Patients with an elongated styloid process might present with dysphagia and pain in the cervicofacial region. These patients could be misdiagnosed as other orofacial pathologies. *Aim*. The present study attempted to assess the prevalence of the elongated styloid process on digital panoramic radiographs in the Riyadh population. *Materials and Methods*. The present prospective randomized study was conducted on the panoramic digital radiographs of 300 randomly selected patients visiting a private dental hospital to identify any elongation of the styloid process. Only the radiographs without any magnification errors were considered. The styloid process length was measured using the Sidexis measuring tool and entered in an Excel spreadsheet with other demographic data. A length beyond 30 mm was considered styloid process elongation. The data were subjected to statistical analysis. *Results*. The symptoms of styloid process elongation were higher among females (78.6%), and this difference was statistically significant ($\chi^2 = 7.182$; $P = 0.007$). No statistically significant association was observed between styloid process elongation and symptoms between different age groups. Females exhibited a significant longer mean length of the styloid process than males. The present study exhibited a 27.3% prevalence for the elongation and calcification of the styloid process. *Conclusion*. Given the significant prevalence of the elongated styloid process in our study, we recommend it to be considered as one of the differential diagnosis for pain or discomfort in the orofacial region.

1. Introduction

The styloid process is a slender bony process starting from the lower portion of the temporal bone anteromedial to the stylomastoid foramen [1]. The term styloid has originated from the Greek word "stylos," which means "pillar" [2]. The process is attached to the lesser cornu of the hyoid bone through the styloid ligament and is flanked on both sides by the external and internal carotid arteries [3]. The normal length of the styloid process is from 15 mm to 30 mm. A length of >30 mm is regarded as elongated [4]. The prevalence of an elongated styloid process in the general population ranges 2%–52% in various studies [5, 6].

The symptomatic elongation of the styloid process is termed as Eagle syndrome. This pathology was first reported in 1937 by the otorhinolaryngologist, Eagle, who termed it stylalgia [7]. Patients with Eagle syndrome present with dysphagia, pain in the cervicofacial region and neck, and pain at the mandibular angle, which aggravate with neck rotation or tongue protrusion. These features may be due to the pressure that the elongated styloid process exerts on the adjacent neurovascular structures [8]. However, the presentation of this pathology may be confusing in a clinical setting and may be misinterpreted as unerupted or impacted tooth, cranial nerve neuralgias, temporal arthritis, temporomandibular joint disorders, migraine, pharyngotonsillitis, and benign and malignant tumors [9, 10]. This may lead to unnecessary invasive diagnostic and therapeutic procedures. Additionally, an elongated styloid process may also cause stroke due to the compression of carotid arteries [11].

Thus, an elongated styloid process must be diagnosed accurately and considered as a differential diagnosis in orofacial pain. Therefore, the present study attempts to evaluate the prevalence of styloid process elongation and its association with demographic factors in the population in Riyadh.

2. Materials and Methods

The present cross-sectional observational study was conducted in 300 patients above 14 years of age in Dar Al Uloom University Hospital, Riyadh, Saudi Arabia, from August 2020 to April 2021, after institutional ethics clearance. The study was conducted according to the guidelines of the Declaration of Helsinki and approved by the Institutional Review Board of College of Dentistry, Dar Al Uloom University, Riyadh, KSA (COD/IRB/2020/5). Both verbal and written consent was obtained from all patients. The patients visiting the dental clinics were randomly selected. Radiographs clearly exhibiting bilateral styloid processes with minimal or no magnification were included in the study. Radiographs exhibiting magnification errors were excluded from the study.

The digital panoramic radiographs of all 300 patients were obtained, and data regarding the same were obtained from the university hospital systems (Sidexis). These panoramic radiographs were taken with a digital panoramic orthophos XG system (Sirona Company) using exposure factors as per manufacturer' instruction. The length of the styloid process was measured from the junction of the process and the tympanic plate to the tip of the process. In case of a segmented styloid process, the measurement was performed in the same manner. The ossification of the stylohyoid or stylomandibular ligaments, if present, was considered a part of the elongated styloid process, and measurements were performed accordingly. A styloid process greater than 30 mm long was considered as elongated.

The patients were interviewed in either Arabic or English depending on their comfort. Extraoral examination was then carried out. The neck region of the patients was palpated for any signs of styloid process elongation. Additional patient information was obtained from the hospital electronic file system (Open Dental). A Sidexis ruler was used to calculate the length of the styloid process in the radiographs (Figure 1).

The data were collected and entered in MS Excel. The results were analyzed using SPSS version 22.0. The association between the different parameters was analyzed using the chi-square test, and $P < 0.05$ was considered statistically significant.

3. Results

The characteristics of the study population are given in Table 1. In the present study, majority of the samples were males ($n = 166$; 55.3%). The majority of patients were in the age group of 20–29 years (34%), followed by 30–39 years (23.3%), 40–49 years (19.3%), above 50 years (12.7%), and less than 20 years (10.7%). The prevalence of elongation and calcification patterns of the styloid process was 27.3% ($n = 82$). Among the patients with positive symptoms ($n = 28$; 9.3%), 4.7% ($n = 14$) exhibited symptoms on the right side and 6% ($n = 18$) exhibited symptoms on the left side. Of these, 4 patients had bilateral symptoms.

Chi-square analysis displayed no statistically significant association among styloid process elongation ($\chi^2 = 4.909$; $P = 0.297$), symptoms ($\chi^2 = 3.357$; $P = 0.5$), and sides of the symptoms ($\chi^2 = 3.78$; $P = 0.706$) with different age groups. Chi-square analysis displayed significantly higher symptoms of styloid process elongation in females (78.6%) compared with males (21.4%) ($\chi^2 = 7.182$; $P = 0.007$). No significant difference was observed in the occurrence of styloid process elongation and symptoms on left and right between males and females ($P > 0.05$).

Table 2 provides the association of styloid process elongation, symptoms, and sides of the symptoms between different age groups. No statistically significant association was observed between styloid process elongation ($\chi^2 = 4.909$; $P = 0.297$), symptoms ($\chi^2 = 3.357$; $P = 0.5$), and sides of the symptoms ($\chi^2 = 3.78$; $P = 0.706$) between different age groups.

Table 3 provides the association of styloid process elongation, symptoms, and sides of the symptoms between males and females. No statistically significant difference was observed between styloid process elongation between males and females ($P > 0.05$). However, the symptoms of styloid process elongation were higher among females (78.6%), and this difference was statistically significant ($\chi^2 = 7.182$; $P = 0.007$).

4. Discussion

Eagle syndrome may cause symptoms such as orofacial pain, which might be confusing to clinicians [8]. All clinicians must be aware of the clinical and radiological signs and symptoms of styloid process elongation to accurately diagnose and treat symptoms in the cervicofacial region. The present study thus attempts to evaluate the prevalence of styloid process elongation in the Riyadh population and its association with demographic factors.

The present study was conducted on digital panoramic radiographs. Numerous imaging modalities can be used for the diagnosis of styloid process elongation. These include modalities such as lateral skull radiograph, Towne's view, anterioposterior skull radiograph, and computed tomography (CT) scan [12]. However, digital panoramic radiographs can be easily performed and interpreted. Additionally, they expose the patients to a lower radiation dose and cost much lesser than CT. Thus, this procedure can be easily used for epidemiological evaluations [13]. Furthermore, digital panoramic radiographs are commonly prescribed for orofacial pain, and a styloid process elongation is usually an accidental finding on these radiographs. So, we opted for this diagnostic modality in the present study.

The present study exhibited a prevalence of 27.3% for the elongation and calcification of the styloid process. This finding was concurrent with those of Bozkir et al., Keur et al.,

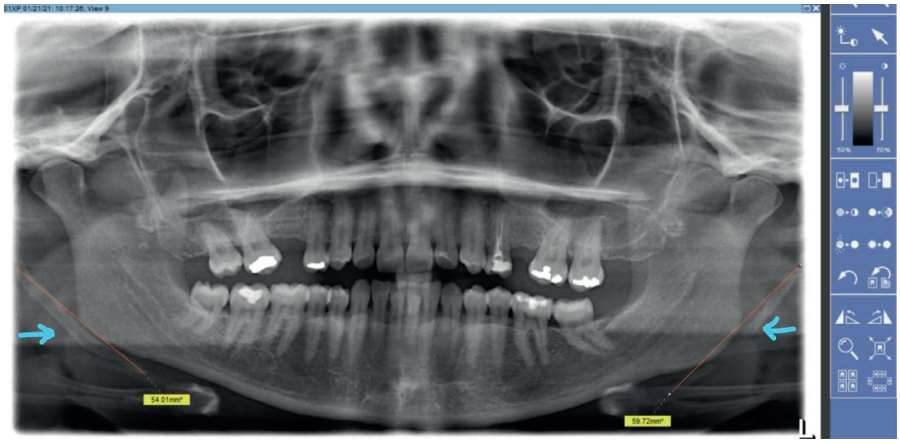

Figure 1: Measuring the elongated styloid process on both sides.

Table 1: Characteristics of the study population.

Age and sex distribution in the population				
			Frequency	%
Age groups	Less than 20 years		32	10.7
	20–29		102	34
	30–39		70	23.3
	40–49		58	19.3
	Above 50 years		38	12.7
Sex	Female		134	44.7
	Male		166	55.3
Mean age among sexes				
		N	Mean age	SD
Sex	Female	134	31.49	11.70
	Male	166	35.47	13.67
Total		300	33.69	12.94
Distribution of elongation of the styloid process				
			Frequency	%
Elongated	No		218	72.7
	Yes		82	27.3
Distribution of symptoms between sides				
			Frequency	%
Symptoms	No		172	90.7
	Yes		28	9.3
Symptoms right	No		286	95.3
	Yes		14	4.7
Symptoms left	No		282	94
	Yes		18	6

N, number of samples; SD, standard deviation.

and Scaf et al., who exhibit prevalence rates less than 30% [14]. However, this finding was in contrast with the findings of AlZarea and Bagga et al. [2, 6]. Bagga et al. reported a prevalence of 52.1% for the elongated styloid process. This difference in prevalence may be explained by the differing geographic area as the study was conducted in Mathura. The authors explained this high prevalence by the fact that majority of the population perform strenuous works such as carrying heavy weights on their heads and chew hard foods such as gutka and areca nut, which may promote the ossification of the ligaments attached to the styloid process [6]. However, the study on AlZ area, exhibiting a prevalence of 43.93% for the elongated styloid process, was conducted in Saudi Arabia itself. However, the population studied was >60 years of age. As the present study included patients as young as 14 years, the age difference in the study population may account for the difference in prevalence.

The difference in the length of the styloid process between different age groups in this study was statistically nonsignificant. This finding was in contrast to the findings of More and Asrani, Bruno et al., and Jamal et al., who reported a progressive increase in the length of the styloid process with aging [12–15]. Additionally, the present study presented a longer mean length of the styloid process in females (right side: 16.04 ± 16.88 mm; left side: 16.44 ± 17.31 mm) compared with males (right side: 12.51 ± 16.38 mm; left side: 13.86 ± 16.89 mm). This finding is in contrast with those of More and Asrani and Jamal et al., who reported longer styloid processes in males as compared with females [12, 15]. However, these findings were concurrent with the findings of Magat and Ozcan, who reported no significant difference in the length of the styloid process between males and females, and Ferrario et al., who reported a longer styloid process length in females [16, 17].

Out of the 34 females with elongated styloid processes in the present study, 22 (78.60%) exhibited symptoms, whereas only 6 (21.40%) of the 48 males with elongated processes exhibited symptoms. This difference was statistically significant ($P = 0.007$). This may be due to the lower pain threshold in females [18].

The present study has certain limitations. Langlais et al. classified the radiographic images of the elongated styloid process into three types based on morphology of elongation, namely, type I: elongated, type II: pseudoarticulated, and type III: segmented [19]. The present study did not take this classification under consideration. The relatively small sample size and the single-centre design of the study prevent the generalization of the findings. Additionally, digital panoramic radiography is prone to magnification errors, which may confound findings. Future multicentre studies with a larger sample size will further strengthen the findings of this study.

Table 2: Association of styloid process elongation, symptoms, and sides of the symptoms between different age groups.

Mean length among age groups (in mm)			
Age groups		Right	Left
Less than 20 years	*N*	32	32
	Mean	13.40	12.73
	SD	17.03	15.03
20–29	*N*	102	102
	Mean	12.85	11.43
	SD	17.01	16.93
30–39	*N*	70	70
	Mean	16.22	19.81
	SD	17.56	18.07
40–49	*N*	58	58
	Mean	13.77	16.69
	SD	15.89	17.14
Above 50 years	*N*	38	38
	Mean	14.54	15.15
	SD	16.06	16.23
Total	*N*	300	300
	Mean	14.09	15.01
	SD	16.64	17.07

Association of styloid process elongation among different age groups									
			Age groups					χ^2 value	*P* value
			Less than 20 years	20–29	30–39	40–49	Above 50 years		
Elongated	No	*N*	28	70	44	46	30	4.909	0.297
	Yes	*N*	4	32	26	12	8		
Symptoms	No	*N*	30	88	64	52	38	3.357	0.5
	Yes	*N*	2	14	6	6	0		

*Statistical significance set at 0.05; *N*, number of samples; χ^2 value, chi-square value.

Table 3: Association of styloid process elongation, symptoms, and sides of the symptoms between males and females.

Mean length among males and females (in mm)			
Sex		Right	Left
Female	*N*	134	134
	Mean	16.04	16.44
	SD	16.88	17.31
Male	*N*	166	166
	Mean	12.51	13.86
	SD	16.38	16.89
Total	*N*	300	300
	Mean	14.09	15.01
	SD	16.64	17.07

Association of styloid process elongation among males and females						
			Sex		χ^2 value	*P* value
			Female	Male		
Elongated	No	N	100	118	0.234	0.628
	Yes	N	34	48		
Symptoms	No	N	112	160	7.182	0.00[7*]
	Yes	N	22	6		

*Statistical significance set at 0.05; *N*, number of samples; χ^2 value, chi-square value.

5. Conclusion

As styloid process elongation may be an accidental finding during radiographic examination, practitioners must remember to look for the same when patients visit with pain in the cervicofacial region. The present study exhibited a prevalence of 27.3% for the elongation and calcification of the styloid process. Thus, it must be considered as a differential diagnosis for pain or discomfort in the orofacial region.

Data Availability

The data used to support the findings of this study are available from the corresponding author upon request.

Ethical Approval

The study was conducted according to the guidelines of the Declaration of Helsinki and approved by the Institutional

Review Board of College of Dentistry, Dar Al Uloom University, Riyadh, KSA (COD/IRB/2020/5).

Consent

Informed consent was obtained from all subjects involved in the study.

Conflicts of Interest

The authors declare that they have no conflicts of interest.

Authors' Contributions

A.L conceptualized, collected resources, visualized, reviewed, and edited the study. A.L, A.A, P.K, and N.A developed methodology. N.A, A.A, and A.L developed software, validated and investigated the study, and wrote the original draft. N.A and A.A performed formal analysis. A.L and P.K involved in data curation and supervised the study. All authors have read and agreed to the published version of the manuscript.

Acknowledgments

The authors extend their appreciation to the Deanship of Postgraduate and Scientific Research at Dar Al Uloom University, Riyadh, KSA, for supporting this work.

References

[1] S. Standring, *Gray's Anatomy the Anatomical Basis of Clinical Practice*, Elsevier, Amsterdam, Netherlands, 39th edition, p. 470, 2005, Skull and Mandible.

[2] B. K. AlZarea, "Prevalence and pattern of the elongated styloid process among geriatric patients in Saudi Arabia," *Clinical Interventions in Aging*, vol. 12, no. 30, pp. 611–617, 2017.

[3] Iannucci, M. Joen, and L. Jansen Howerton, *Dental Radiography: Principles and Techniques*, Elsevier, St. Louis, Missouri, 2017.

[4] J. Alkhabuli, H. Zakaria, and A. Muayad, "Prevalence of stylohyoid complex elongation among patients attending RAK College of dental sciences clinic," *Acta Stomatologica Croatica*, vol. 54, no. 1, pp. 60–68, 2020.

[5] E. M. Vieira, O. A. Guedes, S. D. Morais, C. R. Musis, P. A. Albuquerque, and Á. H. Borges, "Prevalence of elongated styloid process in a central Brazilian population," *Journal of Clinical and Diagnostic Research: JCDR*, vol. 9, pp. ZC90–ZC92, 2015.

[6] M. B. Bagga, C. A. Kumar, and G. Yeluri, "Clinicoradiologic evaluation of styloid process calcification," *Imaging Science in Dentistry*, vol. 42, no. 3, pp. 155–161, 2012.

[7] W. W. Eagle, "Elongated styloid processes: report of two cases," *Archives of Otolaryngology-Head and Neck Surgery*, vol. 25, no. 5, pp. 584–587, 1937.

[8] D. Raina, R. Gothi, and S. Rajan, "Eagle syndrome," *Indian Journal of Radiology and Imaging*, vol. 19, no. 02, pp. 107-108, 2009.

[9] M. A. Baseer and M. S. Alenazy, "Eagle's syndrome: a rare case of young female," *Dental Research Journal*, vol. 10, pp. 568–570, 2013.

[10] G. Krennmair and E. Piehslinger, "Variations of ossification in the stylohyoid chain," *Cranio*, vol. 21, no. 1, pp. 31–37, 2003.

[11] F. Asutay, N. F. Erdem, Y. Atalay, A. H. Acar, and H. Asutay, "Prevalence of elongated styloid process and eagle syndrome in east eagean population," *Bezmialem Science*, vol. 7, no. 1, pp. 28–32, 2019.

[12] C. B. More and M. K. Asrani, "Evaluation of the styloid process on digital panoramic radiographs," *The Indian Journal of Radiology & Imaging*, vol. 20, no. 4, pp. 261–265, 2010.

[13] G. Bruno, A. De Stefani, P. Balasso, S. Mazzoleni, and A. Gracco, "Elongated styloid process: an epidemiological study on digital panoramic radiographs," *Journal of Clinical and Experimental Dentistry*, vol. 9, no. 12, pp. e1446–52, 2017.

[14] G. Scaf, D. Q. d. Freitas, and L. d. C. M. Loffredo, "Diagnostic reproducibility of the elongated styloid process," *Journal of Applied Oral Science*, vol. 11, no. 2, pp. 120–124, 2003.

[15] B. T. Jamal, K. K. Ravikumar, S. H. Alyawar et al., "Prevalence of elongated styloid process and elongation pattern on digital panoramic radiographs in Saudi Population, Jeddah," *International Journal of Psychosocial Rehabilitation*, vol. 3, pp. 37–39, 2018.

[16] G. Magat and S. Ozcan, "Evaluation of styloid process morphology and calcification types in both genders with different ages and dental status," *Journal of Istanbul University Faculty of Dentistry*, vol. 51, no. 2, pp. 29–36, 2017.

[17] V. F. Ferrario, D. Sigurta, A. Daddona et al., "Calcification of the stylohyoid ligament: incidence and morphoquantative evaluation," *Oral Surgery, Oral Medicine, Oral Pathology*, vol. 69, no. 4, pp. 524–529, 1990.

[18] W. G. Lombana, S. E. G. Vidal, and G. Vida, "Pain and gender differences: a clinical approach," *Colombian Journal of Anesthesiology*, vol. 40, no. 3, pp. 207–212, 2012.

[19] R. P. Langlais, D. A. Miles, and M. L. Van Dis, "Elongated and mineralized stylohyoid ligament complex: a proposed classification and report of a case of Eagle's syndrome," *Oral Surgery, Oral Medicine, Oral Pathology*, vol. 61, no. 5, pp. 527–532, 1986.